NJC

Accepted Manuscript

This is an *Accepted Manuscript*, which has been through the Royal Society of Chemistry peer review process and has been accepted for publication.

Accepted Manuscripts are published online shortly after acceptance, before technical editing, formatting and proof reading. Using this free service, authors can make their results available to the community, in citable form, before we publish the edited article. We will replace this *Accepted Manuscript* with the edited and formatted *Advance Article* as soon as it is available.

You can find more information about *Accepted Manuscripts* in the Information for Authors.

Please note that technical editing may introduce minor changes to the text and/or graphics, which may alter content. The journal's standard Terms & Conditions and the Ethical guidelines still apply. In no event shall the Royal Society of Chemistry be held responsible for any errors or omissions in this *Accepted Manuscript* or any consequences arising from the use of any information it contains.

ROYAL SOCIETY OF CHEMISTRY

www.rsc.org/njc

Facile One-pot Assembly of Adhesive Phenols/Fe^{III}/PEI Complexes for Preparing Magnetic Hybrid Microcapsules

Yang Wang, Yun Zhang*, Chen Hou, Fu He, Mingzhu Liu*

State Key Laboratory of Applied Organic Chemistry, Key Laboratory of Nonferrous Metal Chemistry and Resources Utilization of Gansu Province, College of Chemistry and Chemical Engineering, Institute of Biochemical Engineering and Environmental Technology, Lanzhou University, Lanzhou 730000, China

Abstract Magnetic organic-inorganic hybrid microcapsules coordinated of plant phenols, polyethylenimine (PEI) and Fe^{III} ions complexes were prepared in a facile one-pot way. Porous $CaCO_3$ microparticles were used as the hard template for the adsorption of negatively charged Fe_3O_4 nanoparticles, which acted as the source of magnetism for recycled use. Moreover, the coated Fe_3O_4 nanoparticles also helped to improve the rigidness of the microcapsules away from rupture during multiple reuses. Upon addition of tannic acid (TA), PEI and Fe^{III} ions, the magnetic $CaCO_3$ microparticles were coated with the adhesive complexes through chemical chelation and covalent bonding. Then the template was removed using EDTA to construct the target microcapsules. During the $CaCO_3$ formation step, *Candida Rugosa* Lipase (CRL) was used as the biomolecule which was encapsulated in the $CaCO_3$ microparticles. Characterizations demonstrated the as-prepared magnetic microcapsules showed robust structure so that enzyme inside can be protected physically. As a result, the magnetic hybrid microcapsules exhibited high efficiency in

*Corresponding authors. Fax: 86-931-8912113; E-mail address: zhangyun@lzu.edu.cn (Y. Zhang)

*Corresponding author. Fax: 86-931-8912582; E-mail address: mzliu@lzu.edu.cn (M.Z. Liu)

enzyme catalysis and stability against environment due to the high biocompatibility and robust structure.

1. Introduction

Naturally occurring phenols and polyphenols, which can assemble into functional materials for organic-inorganic hybrid construction, are leading advances in materials design and application.[1-3] A salient feature of the natural-joined hybrid materials is the inheritance of the essential properties of the organic and inorganic component, creation of hierarchical structures and functionality with synergistic merits via various building blocks.[4] As ideal ingredients to form natural-joined hybrid materials, families of plant phenols such as epigallocatechin gallate (EGCG), epicatechin gallate (ECG), epigallocatechin (EGC), and tannic acid (TA)[5] which display antioxidant, antibacterial, antimicrobial, antimutagenic, and anticarcinogenic properties have been developed for scientific inspiration due to their strong solid-liquid interfacial activity. For example, the high dihydroxyphenyl (catechol) and trihydroxyphenyl (gallic acid, GA) content of TA has strong affinity towards surfaces.[2,6] Although inspired by the mussel protein, polydopamine (PDA) has attracted interest in the same field because it is simple for substrate coating and modification,[7] the high costs and the characteristically dark color of PDA coatings may be impediments for some practical applications. Thus, TA has been prominent constituent for organic-inorganic film construction due to the desirable properties, such as high mechanical and thermal stability, pH-responsive disassembly, nontoxicity, and hundredfold less costly than dopamine.[2,6,8]

Due to the unique structural properties, TA can make familiar interactions with a

variety of materials to form metal-organic films via multiple reaction pathways, including electrostatic interactions, hydrogen bonding, hydrophobic interactions, and like many other polyphenols, metal chelation.[9-11] Recently, Guo et al. reported the engineering of metal-phenolic networks to introduce a library of metal-phenolic motif materials, which provided an extensive field for the study and application of metal-organic films.[8] As has been proved, the coordination between TA and Fe^{III} ions, is fast (in seconds), structurally rigid and highly biocompatible, forming a TA-Fe^{III} film with desired properties such as high biocompatibility, facile degradability, cyto-protectability and second-step functionality.[2]

Enzyme is superior over chemical catalyst because of its high effectiveness, high specificity, and green reaction conditions.[12] Among the enzymes applied in biocatalyst, lipases [E.C. 3.1.1.3] have been widely studied due to their "interfacial activation" feature when catalyze the hydrolysis of carboxylic acid esters to carboxylic acids and alcohols, and the reactions of chemo-, regio- and stereoselective esterification or trans-esterification under micro/non-aqueous conditions in an efficient and specific way.[13,14] However, the industrial application of enzyme still remains many challenges due to the low stability, high cost, difficult recycling and regeneration. As a very promising strategy, immobilization of enzyme shows lots of advantages involving enhancing the catalytic stability, feasibility for continuous operations, recycling the enzyme and significant reduction of costs and so on.[15] As a result, we dedicated to utilize natural phenols (TA) and inorganic materials (Fe^{III} ions and magnetic Fe_3O_4 nanopaticles) to explore a high efficiency and time-saving method with a novel and

much simpler route for the construction of enzyme reactors.

Herein, efforts were made to construct enzyme microcapsules using low-cost plant polyphenols (TA), polyethylenimine (PEI) and inorganic materials (Fe^{III} ions and magnetic Fe_3O_4 nanopaticles) as precursors for the formation of Fe_3O_4/TA-Fe^{III}-PEI hybrid microcapsules. More specifically, Fe_3O_4 nanoparticles were adsorbed on porous $CaCO_3$ microparticles; then the organic-inorganic hybrid layer was formed in a one-pot step through chelation of TA and Fe^{III} ions and the Schiff base reaction between TA and PEI. At last, $CaCO_3$ templates were removed and the Fe_3O_4/TA-Fe^{III}-PEI hybrid microcapsules were prepared. During the film formation process, covalent binding between PEI and TA could improve the toughness of the hybrid film than sole chelation of TA and metal ions. The magnetic hybrid microcapsules could respond to external magnetic field stimuli for the practical application importance related to enzyme recycle and reuse. Furthermore, the incorporated Fe_3O_4 nanoparticles also helped to retain an intact and rigid structure. In particular, compared to the wide application of polydopamine films, plant polyphenol-inspired coatings not only retain many of the advantages of polydopamine and deposit under similar conditions, but also are colorless and derived in some cases from reagents hundredfold less costly than dopamine. *Candida Rugosa* Lipase (CRL) was immobilized in the microcapsules accompanied with $CaCO_3$ templates formation, the catalytic activity and stability were then investigated in detail.

2. Materials and methods

2.1 Materials

$FeCl_3 \cdot 6H_2O$ and $FeCl_2 \cdot 4H_2O$ were purchased from AiHua Fine Chemicals Co., Ltd. (China); polyethylenimine (PEI, MW *ca.* 800), *Candida rugosa* lipase (CRL, Type VII) and *Bovine serum albumin* (BSA) were purchased from Sigma Chemical Co.; ethylenediamine tetraacetic acid disodium (EDTA), hydrochloric acid (HCl), and other chemicals and reagents were analytical grade, obtained from Tianjing Chemical Reagent Company (China).

2.2 Preparation of Fe_3O_4/TA-Fe^{III}-PEI hybrid microcapsules

Citric acid coated Fe_3O_4 nanoparticles and Fe_3O_4-$CaCO_3$ microparticles were prepared according to our previous report.[16] For the adhesive coating, Fe_3O_4 doped $CaCO_3$ microparticles (10 mg ml^{-1}) were suspended in deionized water which comprised of a mixture of Fe^{III} ions (0.2 or 0.4 mg ml^{-1}), TA(0.8 or 1.6 mg ml^{-1}) and PEI (0.4, 0.8, or 1.6 mg ml^{-1}) under gental stirring. Twenty seconds later, the microparticles were collected by an extenal magnetic field, and washed with deionized water. At last, the Fe_3O_4/TA-Fe^{III}-PEI hybrid microcapsules were obtained after removal of $CaCO_3$ templates with 0.1 M EDTA solution at room tempreture. The Fe_3O_4/TA-Fe^{III} hybrid microcapsules were also prepared under the same condition without PEI addition.

2.3 Assay of CRL immobilization

2.3.1 CRL immobilization

CRL doped $CaCO_3$ microparticles were prepared as followed: a certain amount of CRL was dissolved in 1 ml of phosphate buffer solution (0.1 M, pH 7.0), and then added into 4 ml $CaCl_2$ solution (final $CaCl_2$ concentration was 0.33 M).

Fe_3O_4/TA-Fe^{III} hybrid microcapsules immobilized CRL was prepared following the same procedure described as above (section 2.2). Especially, after CRL was encapsulated into $CaCO_3$ microparticles, the $CaCO_3$ immobilized CRL was filtered off and quantitatively washed with phosphate buffer solution (0.1 M, pH 7.0) several times to remove the unreacted CRL. The reaction solution and washing solution were collected to assay the amount of residual lipase.

2.3.2 Determination of Immobilization Efficiency and Lipase Activity

The immobilization efficiency was expressed by the amounts of enzyme bounded on supports of unite mass, and the amount of enzyme was determined by the Bradford method,[17] using BSA as the standard. The enzymatic activities of free and immobilized lipase were measured by the titration of the fatty acid which comes from the hydrolysis of olive oil[14] and reverse titration was adopted. One unit of lipase activity (U) is defined as the amount of enzyme needed to hydrolyze olive oil liberating 1.0 μmol of fatty acid per min in the assay condition.

The efficiency of immobilization was evaluated in terms of activity yields and immobilization yield as follows:

activity yield (%) = $\frac{C}{A}100\%$

immobilization yield (%) = $\frac{A-B}{A}100\%$

Where A is the activity of lipase added in the initial immobilization solution, B is the total activity of the residual lipase in the immobilization and washing solution after the immobilization procedure, and C is the activity of the immobilized lipase, respectively.

The relative activity (%) is the ratio between the activity of every sample and the maximum activity of the sample.

The residual activity (%) is the ratio between the activity of each sample and the initial activity of the sample.

All data used in these formulas are the average of triplicate of experiments.

2.3.3 Effect of pH, temperature and thermal stability of free and immobilized lipase activities

A certain amount free and the immobilized CRL were incubated in phosphate buffer (0.1 M, pH 3.0-9.0) by hydrolysis of olive oil in a water bath at 37 ℃ for 30 min with continuous stirring, respectively. Then the enzymatic activities were determined and the relative activity was calculated.

The effect of temperature on the catalytic activities of free and the immobilized CRL were measured by hydrolysis of olive oil in a water bath at 37 ℃ for 30 min, after they were first incubated in phosphate buffer (0.1 M, pH = 7.0) among the temperature range of 20-90 ℃ for 30 min. The relative activity was compared.

Thermal stabilities of the free and the immobilized CRL were determined by measuring the activities after incubated in phosphate buffer (0.1 M, pH = 7.0) at 50 ℃ for 240 min with continuous stirring. A sample was removed with 30 min interval and tested for enzymatic activity. The residual activity was calculated as above.

2.3.4 Reusability

The reusability of Fe_3O_4/TA-Fe^{III}-PEI encapsulated CRL was determined by hydrolysis of olive oil with the recovered lipase which was magnetic separated and

thoroughly washed with phosphate buffer (0.1 M, pH 7.0). Finally, the activities of the subsequent enzymatic reaction were compared with that of the first running (relative activity defined as 100%).

2.3.5 Kinetic Parameters (K_m and V_{max}) of free and immobilized CRL

The Michaelis constant (K_m) and the maximum reaction velocity (V_{max}) of free and Fe_3O_4/TA-Fe^{III}-PEI immobilized CRL were determined by measuring initial rates of the hydrolysis reaction in phosphate buffer (0.1 M, pH 7.0) at 37 °C. Equivalent free or the immobilized CRL was added into olive oil emulsification solution with different concentrations from 0.4-2.0 mg ml^{-1}, and the reaction was carried out for 5 min to determine enzymatic activities. K_m and V_{max} for the free and immobilized CRL were calculated using the Michaelis-Menten model:

$$\frac{1}{V} = \frac{K_m}{V_{max}} \times \frac{1}{[S]} + \frac{1}{V_{max}}$$

where V (U mg^{-1}) was the initial reaction rate, [S] (ml mg^{-1}) was the initial substrate concentration, V_{max} (U mg^{-1}) was the maximum reaction rate obtained at infinite initial substrate concentration, and K_m (mg ml^{-1}) was the Michaelis-Menten contant.

2.4 Characterization

Fourier transform infrared (FTIR) spectra were obtained in transmission mode on a FTIR spectrometer (American Nicolet Corp. Model 170-SX) using the KBr pellet technique. The morphologies of the samples were characterized by a field-emission scanning electron microscopy (SEM, Hitachi S-4800, Japan) and transmission electron microscope (TEM, FEI Tecnal G^2F30) equipped with energy-dispersive X-ray spectroscopy (EDX, Oxford Instrument). Magnetization measurements were

175 performed on a Vibrating sample magnetometer (LAKESHORE-7304, USA) at room
176 temperature. The surface composition and oxidation state of the samples were
177 performed by the X-ray photoelectron spectroscopy (XPS, ESCALAB210).

178 **3. Result and discussion**

179 **3.1 Preparation and characterization of hybrid microcapsules**

180 Fig. 1a shows the synthesize process of Fe_3O_4/TA-Fe^{III}-PEI hybrid microcapsules,
181 which can be divided into four steps: (1) preparation of $CaCO_3$ microparticles using
182 $CaCl_2$ and $NaCO_3$ aqueous solutions. Thus, biomoleculas (such as enzymes) can be
183 encapsulated into the $CaCO_3$ templates; (2) adsorption of citric acid coated Fe_3O_4
184 nanoparticles by the electrical and physical interactions. Our previous work has
185 reported the mechanism of preparing magnetic $CaCO_3$ template, which negatively
186 charged Fe_3O_4 nanoparticles with a diamer of about 10-15 nm can be adsorbed into
187 the lumen or on the surface of $CaCO_3$ microparticles; (3) coating of organic-inorganic
188 hybrid film on magnetic $CaCO_3$ microparticles with plant phonel (TA), metal ions
189 (Fe^{III}) and PEI via a biomimetic route; (4) removal of $CaCO_3$ sacrifical templates
190 through EDTA treatment. Compared with many other related works for the
191 preparation of organic-inorganic hybrid microcapsules,[18-20] our work aims at design
192 an easily recyclable, low cost and time-saving method for the fabrication of biological
193 capsules. During the outer layer formation process, the galloyl groups from TA can
194 react with Fe^{III} ions to form a octahedral complex, the catechol from TA can be
195 cross-linked with PEI to form hydrogels (Fig.1b),[21] thus the adhesive film can be
196 produced.

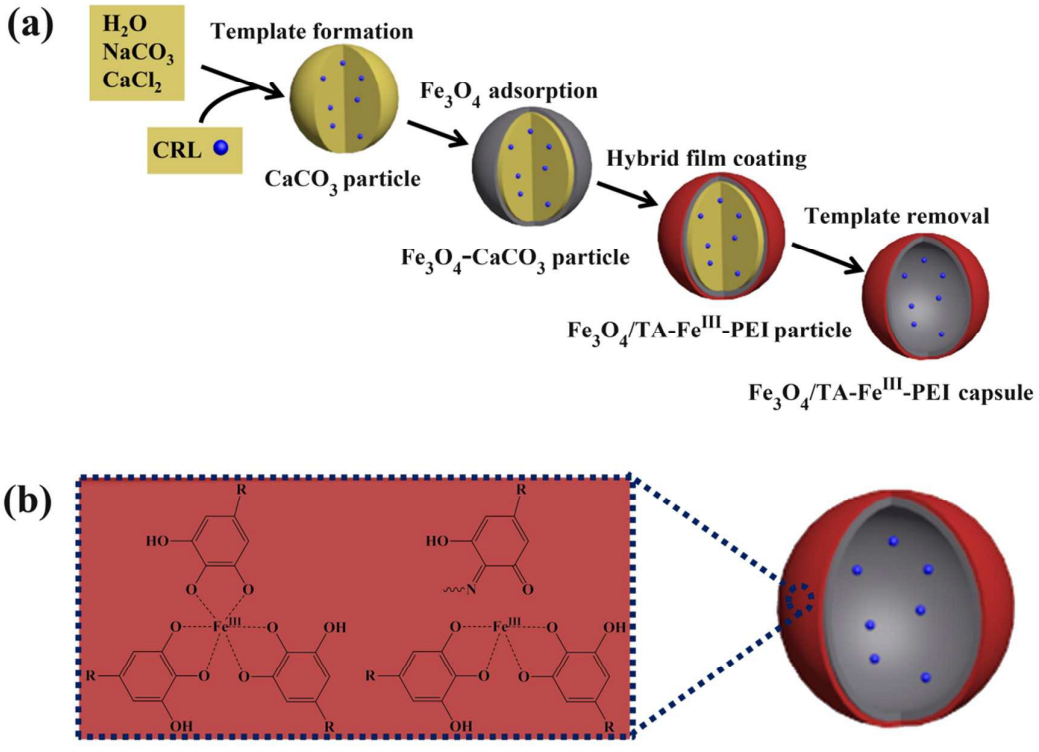

Fig. 1 Schematic illustration of the synthesis process to produce Fe_3O_4/TA-Fe^{III}-PEI microcapsules.

Fig. 2 demenstrated morphologies of the prepared microparticles and microcapsules. As can be seen from Fig. 2 (a1), the as-prepared $CaCO_3$ microparticles possessed uniform, spherical shape with a diameter about 3 μm. After adsorption of Fe_3O_4 nanoparticles, many tiny nanoparticles (with a diameter about 10-15 nm) were assembled on $CaCO_3$ microparticles to cover the original smooth surface (Fig. 2 (a2)), indicating the successful preparation of Fe_3O_4-$CaCO_3$ microparticles. Several batches of Fe_3O_4/TA-Fe^{III}-PEI microcapsules were prepared to vary the concentration of TA, Fe^{III} ions and PEI in the reaction mixtures as followed: TA 0.2 mg ml^{-1}, Fe^{III} ions 0.8 mg ml^{-1} and PEI 0.4 mg ml^{-1} (Fe_3O_4/$TA_{0.2}$-$Fe^{III}_{0.8}$-$PEI_{0.4}$), TA 0.2 mg ml^{-1}, Fe^{III} ions 0.8 mg ml^{-1} and PEI 0.8 mg ml^{-1} (Fe_3O_4/$TA_{0.2}$-$Fe^{III}_{0.8}$-$PEI_{0.8}$), TA 0.4 mg ml^{-1}, Fe^{III}

ions 1.6 mg ml^{-1} and PEI 1.6 mg ml^{-1} (Fe_3O_4/$TA_{0.4}$-$Fe^{III}_{1.6}$-$PEI_{1.6}$). For the comparison, TA 0.2 mg ml^{-1} and Fe^{III} ions 0.8 mg ml^{-1} repeated coating for 3 times was performed (Fe_3O_4/($TA_{0.2}$-$Fe^{III}_{0.8}$)$_3$). As can be seen from Fig.2 (b1), (c1), (d1), and (e1), after coated by the hybrid layer, the microparticles held unifrom surface and spherical structure, which were not affected by the interactions among TA, Fe^{III} ions and PEI. After template removal, the hollowed microcapsules were formed and no obviously collapse appeared. The slight creases of the wall made it a pisiform appearance (Fig.2 (d2), (e2)). The wall of the hybrid microparticles became thicker and rougher with the increase of the coating concentrations, and the spherical morphologies of the hybrid microparticles towards distinct and intact (Fig.2 (b2), (c2), (d2), and (e2)). Besides, it can be clearly observed that Fe_3O_4 nanoparticles were wrapped in the hybrid layer after $CaCO_3$ microparticles dissolution (Fig.2 (f1), (f2)). As for microcapsule Fe_3O_4/($TA_{0.2}$-$Fe^{III}_{0.8}$)$_3$, we also obtained the expected result (Fig.2 (b2)) while it would not be the optimized option for enzyme immobilization due to the weaker wall structure without PEI doping. Thus, it can be verified that the hollow and robust Fe_3O_4/TA-Fe^{III}-PEI microcapsules were successfully achieved.

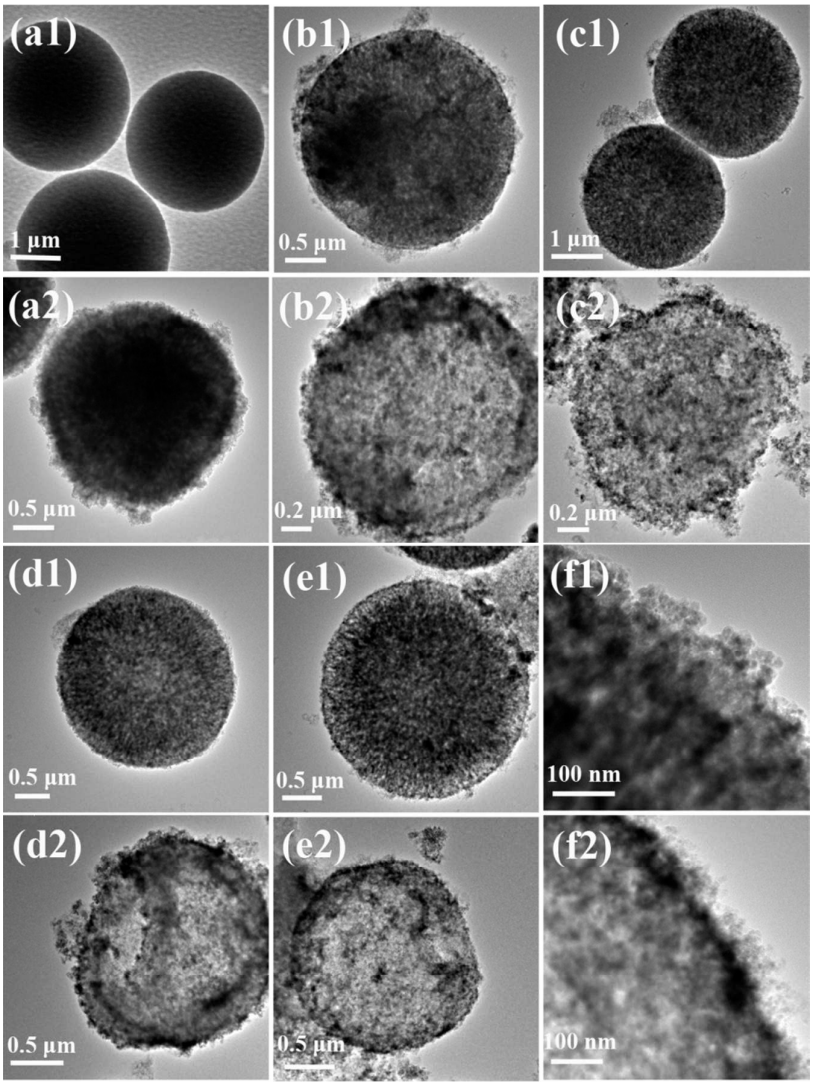

Fig. 2 TEM images of (a1) $CaCO_3$ microparticle, (a2) Fe_3O_4-$CaCO_3$ microparticle, (b1) microparticle, and (b2) microcapsule of $Fe_3O_4/(TA_{0.2}\text{-}Fe^{III}_{0.8})_3$, (c1) microparticle, and (c2) microcapsule of $Fe_3O_4/TA_{0.2}\text{-}Fe^{III}_{0.8}\text{-}PEI_{0.4}$, (d1, f1) microparticle, and (d2, f2) microcapsule of $Fe_3O_4/TA_{0.2}\text{-}Fe^{III}_{0.8}\text{-}PEI_{0.8}$, (e1) microparticle, and (e2) microcapsule of $Fe_3O_4/TA_{0.4}\text{-}Fe^{III}_{1.6}\text{-}PEI_{1.6}$.

To futher observe the surface feature of the microparticles and microcapsules, SEM images were conducted. As shown in Fig. 3, after adsorption of negtively charged Fe_3O_4 nanoparticles, the surface of $CaCO_3$ microparticles became rough and coarse

(Fig. 3 (a), (b)), which was consistent with the TEM images. It futher indicated that the Fe_3O_4 nanoparticles were distributed uniformly on the surface of $CaCO_3$ microparticles. In the cases of the as-prepared hybrid microcapsules, all of them possessed the plump structure due to the inlaid Fe_3O_4 nanoparticles (Fig. 3 (c), (d), (e) and (f)). Moreover, absence or decrease the concentration of PEI would lead to an incompact wall structure (Fig. 3 (c), (d)). If the concentration of TA, Fe^{III} ions and PEI doubled, the superfluous complex was adhered on the side of the microcapsules (Fig. 3 (f)). The uniform and tidy microcapsules were obtained with the premium condition for $Fe_3O_4/TA_{0.2}\text{-}Fe^{III}_{0.8}\text{-}PEI_{0.8}$ (Fig. 3 (e)). In addition, compared with PDA-Fe_3O_4 microcapsules we made,[16] the new prepared Fe_3O_4/TA-Fe^{III}-PEI microcapsules had a more micromesh and homogeneous wall structure attributed to the raqid coating process.

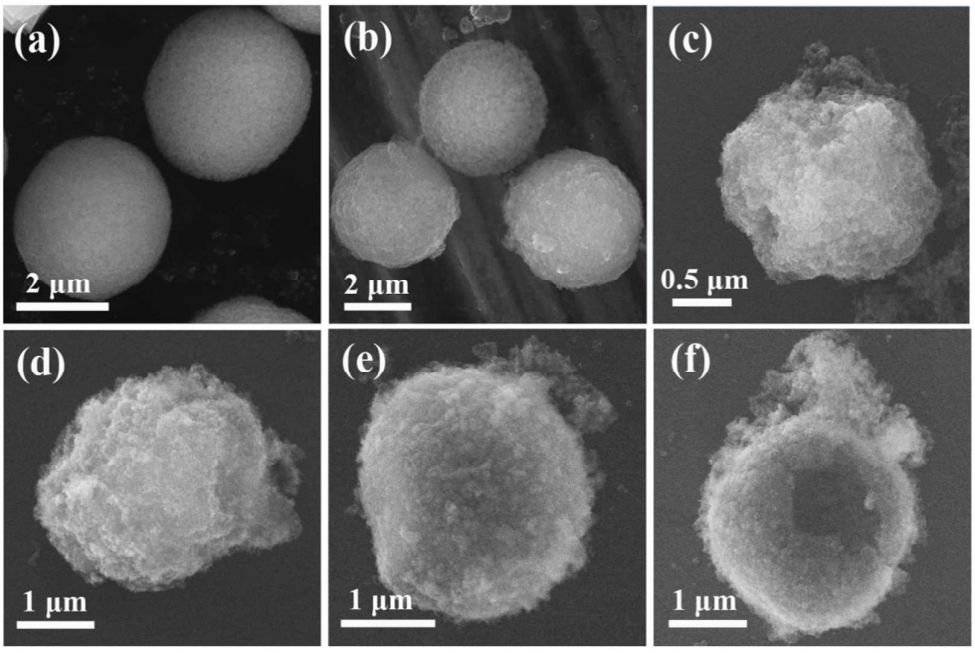

Fig. 3 SEM images of (a) $CaCO_3$ microparticles, (b) Fe_3O_4-$CaCO_3$ microparticles, (c) $Fe_3O_4/(TA_{0.2}\text{-}Fe^{III}_{0.8})_3$ microcapsule, (d) $Fe_3O_4/TA_{0.2}\text{-}Fe^{III}_{0.8}\text{-}PEI_{0.4}$ microcapsule (e)

$Fe_3O_4/TA_{0.2}$-$Fe^{III}_{0.8}$-$PEI_{0.8}$ microcapsule, and (f) $Fe_3O_4/TA_{0.4}$-$Fe^{III}_{1.6}$-$PEI_{1.6}$ microcapsule (damaged-capsules of (f) were made from broken $CaCO_3$ microparticles by grinding and ultrasound of the as-prepared $CaCO_3$ microparticles).

FTIR was conducted to exmaine the functional groups of the prepared magnetic hybrid materials. As shown in Fig. 4a, characteristic peak at 580 cm^{-1} of Fe_3O_4-$CaCO_3$ can be attributed to the lattice absorption of Fe_3O_4 nanoparticles, adsorption bands appearing at 1491/1434 cm^{-1}, 1087 cm^{-1}, and 876 cm^{-1} can be assigned to the vibrations of the carbonate group in $CaCO_3$. In the spectrum of $Fe_3O_4/(TA_{0.2}$-$Fe^{III}_{0.8})_3$, the decreased intensity of the C-OH stretching peak of TA at around 1250 cm^{-1} shown the evidence that the phenolic groups coordinated with Fe^{III} ions.[8] The same situation is also observed in $Fe_3O_4/TA_{0.2}$-$Fe^{III}_{0.8}$-$PEI_{0.8}$ microcapsule. The adsorption peak at 1622 cm^{-1} is attributed to the o-benzoquinone derivative arising from the oxidation of TA[22] which evidenced the rationality of step reaction with PEI. After reacted with PEI, the old peak of $Fe_3O_4/(TA_{0.2}$-$Fe^{III}_{0.8})_3$ at 1622 cm^{-1} disappeared and the new peak of $Fe_3O_4/TA_{0.2}$-$Fe^{III}_{0.8}$-$PEI_{0.8}$ at 1601 cm^{-1} represented the aromatic C=N, which successfully confirmed the reaction between TA and PEI.

To further confirm the reaction phenomenon of the compounds, image of the different reacting mixture was displayed (Fig. 4b). At neutral condition the mixture of Fe^{III} ions and TA solutions transformed into dark blue solution due to the formation of tris-pyrogallato iron complexes. After PEI was added into the above mixture, it turned into sticky prunosus colour immediately. The mixture of TA and PEI was milky white hydrogels as they were mixed immediately. Thus the reactions among Fe^{III} ions, TA

and PEI were proved to be fast visually.

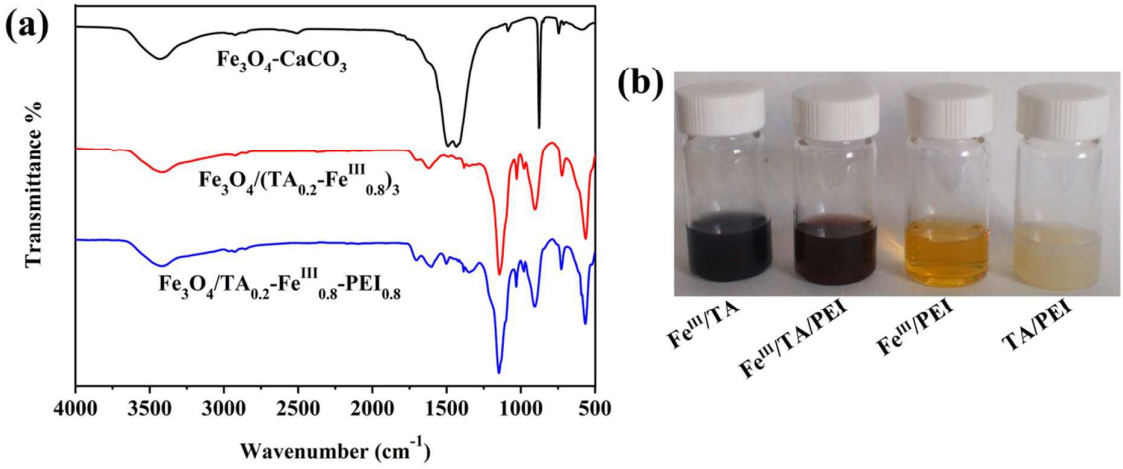

Fig. 4 (a) FTIR spectra of the as-prepared Fe_3O_4-$CaCO_3$ microparticles, $Fe_3O_4/(TA_{0.2}\text{-}Fe^{III}_{0.8})_3$ microcapsules, and $Fe_3O_4/TA_{0.2}\text{-}Fe^{III}_{0.8}\text{-}PEI_{0.8}$ microcapsules, (b) photographs of the physical state of the samples during the vial test.

XPS was performed to identificate the presence of metal ions and PEI in the microcapsule shells (Fig. 5). As displayed in Fig. 5, C1s, O1s, N1s, and Fe2p peaks were detected in the survey spectra, and this is in agreement with the hybrid wall compositions. From the O1s photoelectron apectrum (Fig. 4b), peaks at ~531.29, ~530.07, ~529.18, and ~528.28 eV can be assigned to C=O, C-O, Fe-OH, and Fe-O species, respectively. C=O corresponded to the o-benzoquinone derived from TA and Fe-O/Fe-OH arised from the coordination between TA and Fe^{III} ions. From the N1s spectra (Fig. 4c), peaks appearing at ~399.81, ~397.94, and ~397.37 eV can be attributed to $-NH_2$, -NH-, and -N=, respectively, which suggested the successful chemical crosslinking between TA and PEI.

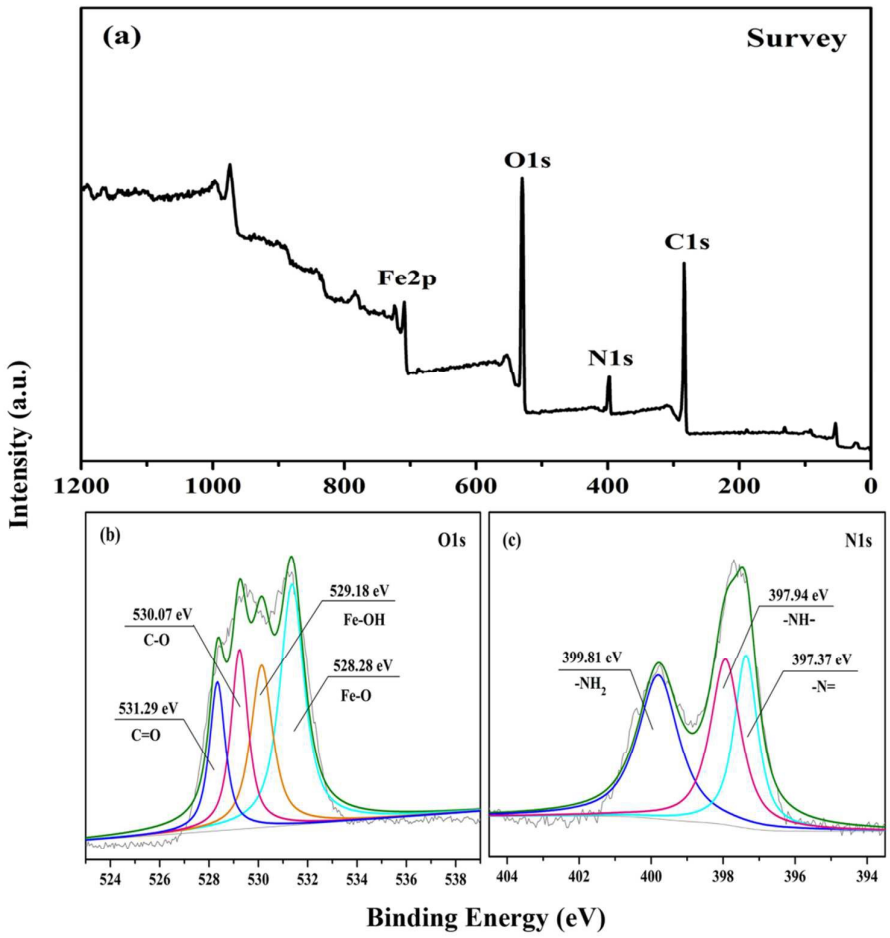

Fig. 5 XPS of $Fe_3O_4/TA_{0.2}$-$Fe^{III}_{0.8}$-$PEI_{0.8}$ microcapsules: (a) survey spectrum, (b) O1s core-level spectrum, and (c) N1s core-level spectrum.

The hysteresis loops of the prepared magnetic nanoparticles are shown in Fig. 6. From Fig. 6 we can see that the saturation magnetization (MS) values are about 66.67 emu g^{-1} for CA-Fe_3O_4 nanoparticles, and 34.69 emu g^{-1} for $Fe_3O_4/TA_{0.2}$-$Fe^{III}_{0.8}$-$PEI_{0.8}$ microcapsules, respectively. As a result, the microcapsules used for CRL immobilization could be separated quickly and easily from the reaction medium with an external field. Compared to the magnetic PDA microcapsules we previously made,[16] the as-prepared microcapsules possessed significantly higher saturation magnetization, and it would obtain an improved efficiency for the immobilized

enzyme recycle and reuse. Furthermore, there are no hysteresis in the magnetization with both remanence and coercivity being zero, indicating that the as-prepared $Fe_3O_4/TA_{0.2}$-$Fe^{III}_{0.8}$-$PEI_{0.8}$ microcapsules are superparamagnetic at room pempreture.[23]

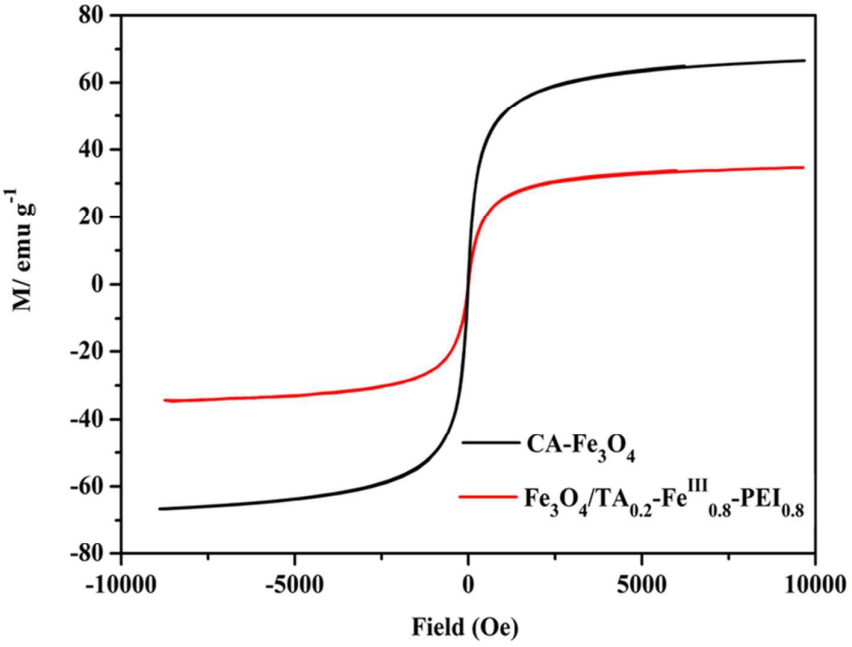

Fig. 6 Magnetic hysteresis loops of CA-Fe_3O_4 nanoparticles, and $Fe_3O_4/TA_{0.2}$-$Fe^{III}_{0.8}$-$PEI_{0.8}$ microcapsules.

3.2 Application of hybrid microcapsules for enzyme immobilization and enzyme catalysis

For the CRL immobilization, $Fe_3O_4/TA_{0.2}$-$Fe^{III}_{0.8}$-$PEI_{0.8}$ microcapsules were used. As shown in Fig. 7, with the increase of CRL concentration, the encapsulation efficiency decreased monotonically and the immobilized enzyme exhibited increased activity, simultaneously. At the enzyme concentration between 1.0 and 1.5 mg ml^{-1}, the relative activity of immobilized CRL reached up to 97%. In addition, to evaluate the enzymatic properites, the kinetics of the immobilized CRL with the concentration of 1.0 mg ml^{-1} in $Fe_3O_4/TA_{0.2}$-$Fe^{III}_{0.8}$-$PEI_{0.8}$ microcapsules were calculated from an

enzymatic assay by Michaelis-Menten enzyme kinetics model (Table 1). As displayed in Table 1, in contrast to free CRL, the higher K_m for CRL-Fe_3O_4/$TA_{0.2}$-$Fe^{III}_{0.8}$-$PEI_{0.8}$ indicated a lower affinity of the CRL towards the substrates because of additional diffusion resistance after encapsulation. The lowered V_{max} for the immobilized CRL indicated that the microencapsulation restricted the activity of enzyme, which was possibly due to the inner diffusion lowered the accessibility of substrates to the active sites on CRL.

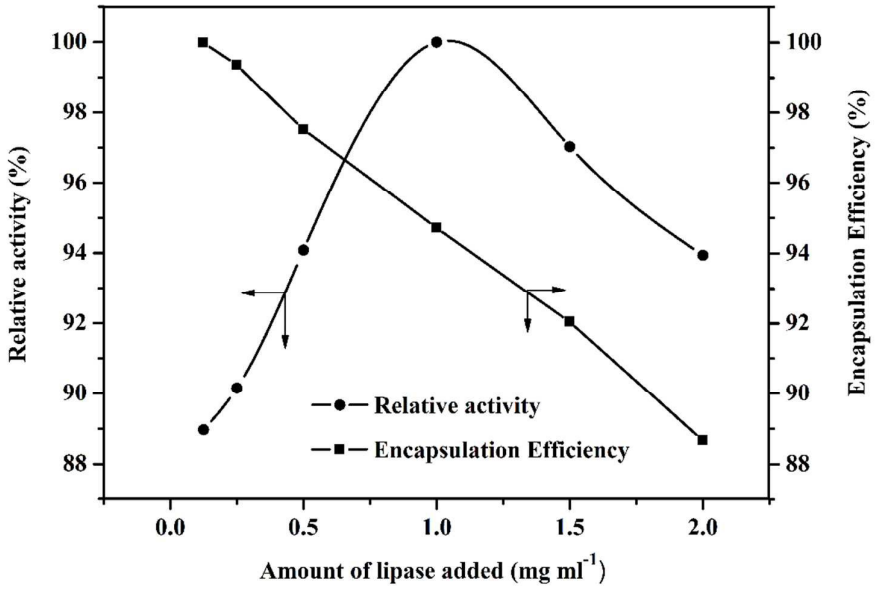

Fig. 7 Effect of enzyme amount and encapsulation efficiency of Fe_3O_4/$TA_{0.2}$-$Fe^{III}_{0.8}$-$PEI_{0.8}$ microcapsules.

Table 1. Kinetic Parameters of free CRL and CRL-Fe_3O_4/$TA_{0.2}$-$Fe^{III}_{0.8}$-$PEI_{0.8}$ microcapsules.

	K_m (mg ml^{-1})	V_{max} (U mg^{-1})
Free CRL	0.43	6.05
CRL-Fe_3O_4/$TA_{0.2}$-$Fe^{III}_{0.8}$-$PEI_{0.8}$	0.54	5.10

The pH stability of CRL-Fe_3O_4/$TA_{0.2}$-$Fe^{III}_{0.8}$-$PEI_{0.8}$ microcapsules and free CRL are compared in Fig. 8a. The CRL-Fe_3O_4/$TA_{0.2}$-$Fe^{III}_{0.8}$-$PEI_{0.8}$ kept >71% of its initial activity at pH 5.0-8.0, a decline below pH 4.0 and above 9.0. In comparison, the free CRL retained 29% of the relative activity at pH 3.0 and 42% of the relative activity at pH 9.0. In addition, CRL-Fe_3O_4/$TA_{0.2}$-$Fe^{III}_{0.8}$-$PEI_{0.8}$ showed broader pH scope. As a result, the Fe_3O_4/$TA_{0.2}$-$Fe^{III}_{0.8}$-$PEI_{0.8}$ used for CRL immobilization exhibited markedly improved adaptability in a wide pH range, which can greatly expand the applications of lipase in chemical and biocatalytic industries. This phenomenon can be explained by the buffering effect of the hybrid layer of the microcapsules. The abundant -OH/$-O^-$ pairs on TA and the $-NH_2$/$-NH_3^+$ pairs on PEI could tune the local pH value under basic or acidic conditions. Therefore, the CRL near the hybrid walls would stay in the buffer region against the environmental mutation to maintain the activity of the CRL due to the positive influence of TA and PEI ingredients.

When the hydrolysis for olive oil emulsion was operated at a series of temperature range, the immobilized CRL showed enhanced relative activities than the free CRL (Fig. 8b). Compared with free lipase, the immobilized CRL kept its relative activity up to 80% in the temperature range of 20-60 °C and exhibited more than 60% of relative activity at 90 °C, revealed much superber heat endurance than that of the free lipase. It seemed that the interaction between the positively charged PEI and negatively charged CRL molecules would conduct a tough performance with enzymes from denaturation at high temperatures.[24]

The strong thermal stability is one of the critical factors in the industrial

348 applications. Fig. 8c shows the residual activity of free and immobilized lipase at
349 50 °C on the hydrolysis reaction of olive oil. From Fig. 8c we can see, after incubated
350 for 150 min, free CRL lost the activity while immobilized CRL retained the residual
351 activity as high as 58% until the incubate time reached 240 min. This phenomenon
352 probably resulted from the excellent thermal stability, good mechanical hardness and
353 well biocompatibility of the prepared organic-inorganic hybrid microcapsules, which
354 protected the CRL from unfolding and conformational transitions.

355 The well reusability of lipase is critical for the potential application in industry. As
356 presented in Fig. 8d, the immobilized enzyme kept the high activity at 75% after 12
357 times reuse due to the sturdy stability of the hybrid microcapsules which effectively
358 ameliorated the denaturation and leakage of enzyme under multiple reaction circles.
359 Moreover, the loss of microcapsules during each recycle cannot be ignored. As a
360 result, the layer assemblied by Fe_3O_4 and TA-Fe^{III}-PEI had a high biocompatibility
361 and strong mechanical property which could effectively mitigate the deactivation,
362 leaching and embedding of the encapsulated enyzmes.

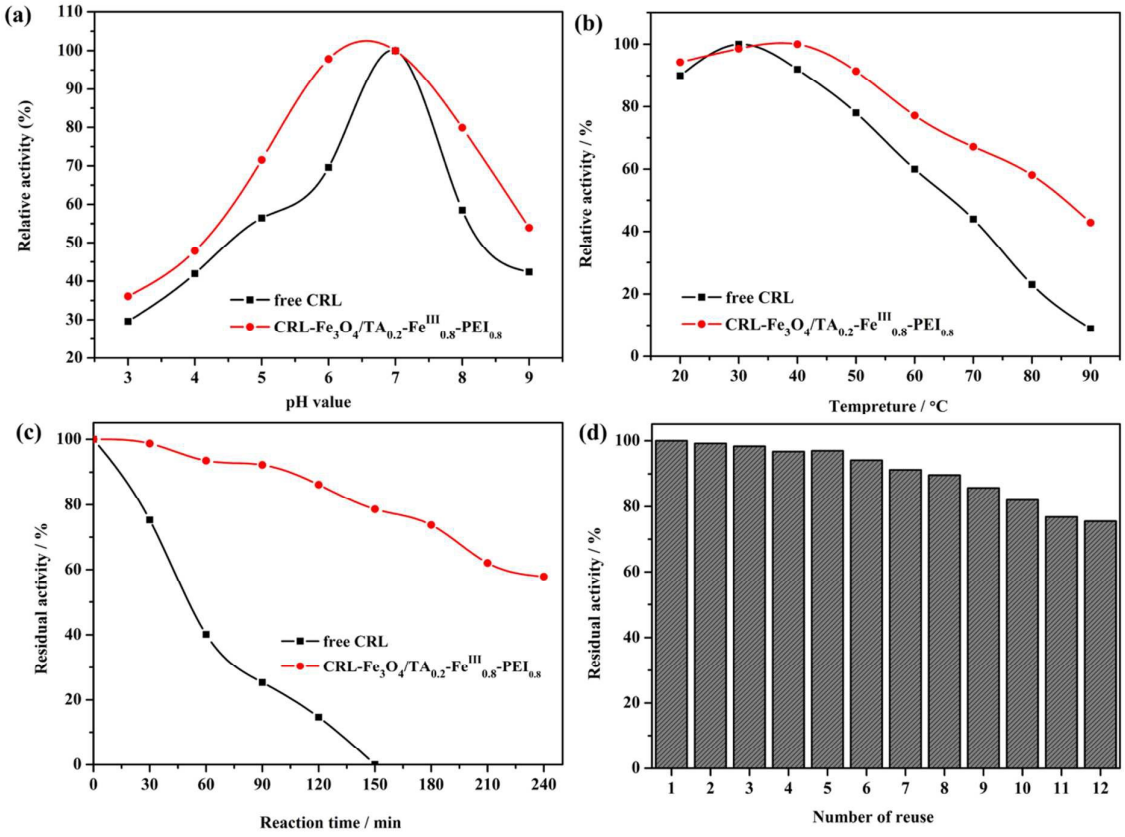

Fig. 8 Effect of (a) pH value, (b) temperature, (c) stability, and (d) number of reuse of free and immobilized CRL.

4. Conclusion

A facile and easy method was developed to prepare magnetic metal-polyphenol-polyethylenimine hybrid microcapsules by combining plant phenols chelating with covalent bonding. The hybrid wall with negligible cytotoxicity provided an appropriate environment for the enzyme inside. Plant phonels (tannic acid) constructed microcapsule walls exhibited excellent characteristics such as high biocompatibility, second-step functionality, colorless, low cost and time-saving (in seconds). Meanwhile, the polyethylenimine motifs in the hybrid layer are in charge of enhancing the toughness of the hybrid layer. Significantly, the incorporated Fe_3O_4

nanoparticles acted practical dual role in the microcapsule formation and application; both the recyclable ingredient and the powerful skeleton to retain the intact, rigid, hollowed structure during the multiple-reuse. The formulated hybrid magnetic microcapsules exhibited high encapsulation efficiency for *Candida Rugosa* Lipase and improved activity in catalysis compared with the free lipase. Therefore, the method we introduced may be extend to prepare many other hybrid materials and applied in bio-fields.

Acknowledgment

The authors thank the financial supports from the National Natural Science Foundation of China (No.21374045, No.21074049). This paper is dedicated to memory of pro. Yanfeng Li, who passed away recently.

References

1. H. Lee, N. F. Scherer and P. B. Messersmith, *Proc. Natl. Acad. Sci.* 2006, **103**, 12999-13003.
2. T. S. Sileika, D. G. Barrett, R. Zhang, K. H. A. Lau and P. B. Messersmith, *Angew. Chem. Int. Ed.* 2013, **52**, 10766 -10770.
3. E. Haslam, *Cambridge University Press* 1998.
4. C. Y. Tian, C. H. Zhang, H. Wu, Y. X. Song, J. F. Shi, X. L. Wang, X. K. Song, C. Yang and Z. Y. Jiang, *J. Mater. Chem. B*, 2014, **2**, 4346-4355.
5. T. J. Kim, J. L. Silva, M. K. Kim, Y. S. Jung and *Food Chem.* 2010, **118**, 740-746.
6. H. Ejima, J. J. Richardson, K. Liang, J. P. Best, M. P. Koeverden, G. K. Such, J. W. Cui and F. Caruso, *Science* 2013, **341**, 154-157.
7. Y. L. Liu, K. L. Ai and L. H. Lu, *Chem. Rev.* 2014, **114**, 5057-5115.
8. J. L. Guo, Y. Ping, H. Ejima, K. Alt, M. Meissner, J. J. Richardson, K. Peter, D. Elverfeldt, C. E. Hagemeyer and F. Caruso, *Angew. Chem. Int. Ed.* 2014, **53**, 5546-5551.
9. H. I. Oh, J. E. Hoff, G. S. Armstrong and L. A. Haff, *J. Agr. Food Chem.* 1980, **28**, 394-398.
10. E. Costa, M. Coelho, L. M. Ilharco, A. Aguiar-Ricardo and P. T. Hammond, *Macromolecules* 2011, **44**, 612-621.
11. T. Shutava, M. Prouty, D. Kommireddy and Y. Lvov, *Macromolecules* 2005, **38**, 2850-2858.

12. J. Garcia, Y. Zhang, H. Taylor, O. Cespedes, M. E. Webb and D. J. Zhou, *Nanoscale* 2011, **3**, 3721-3730.

13. K. Jaeger, M. Reetz, *Trends. Biotechnol.* 1998, **16**, 396-403.

14. Y. Omprakash, I. Toyoko, *Biomacromolecules* 2005, **6**, 2809-2814.

15. X. Liu, X. Chen, Y. F. Li, X. Y. Wang, X. M. Peng and W. W. Zhu, *ACS Appl. Mater. Interfaces* 2012, **4**, 5169-5178.

16. C. Hou, Y. Wang, H. Zhu and L.C. Zhou, *J. Mater. Chem. B* 2015, 3, 2883-2891.

17. M.M. Bradford, *Anal. Biochem.* 1976, **72**, 248-254.

18. J. F. Shi, W. Y. Zhang, S. H. Zhang, X. L. Wang and Z. Y. Jiang, *J. Mater. Chem. B* 2015, **3**, 465-474.

19. W. Y. Zhang, J. F. Shi, X. L. Wang, Z. Y. Jiang, X. K. Song and Q. H. Ai, *J. Mater. Chem. B* 2014, **2**, 1371-1378.

20. X. L. Wang, Z. Y. Jiang, J. F. Shi, Y. P. Liang, C. H. Zhang and H. Wu, *ACS Appl. Mater. Interfaces* 2012, 4, 3476-3483.

21. M. Krogsgaard, A. Andersen and H. Birkedal, *Chem. Commun.* 2014, 50, 13278-13281.

22. A. Dutta, S. K. Dolui, *Appl. Surf. Sci.* 2011, 257, 6889-6896.

23. K. E. Mooney, J. A. Nelson and M. Wagner, *Chem. Mater.* 2004, **16**, 3155-3161.

24. X. L. Wang, J. F. Shi, Z. Li, S. H. Zhang, H. Wu, Z. Y. Jiang, C. Yang and C. Y. Tian, *ACS Appl. Mater. Interfaces* 2014, **6**, 14522-14532.

Graphical abstract:

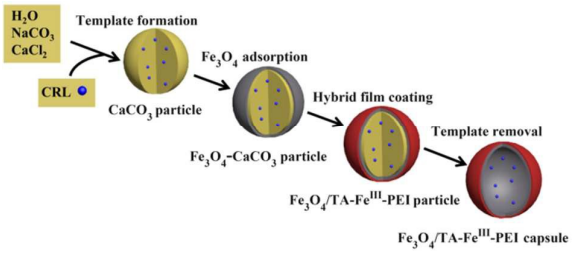

Magnetic organic-inorganic hybrid microcapsules coordinated of plant phenols, polyethylenimine and Fe^{III} ions complexes were prepared in a facile one-pot way.